

Observed Tropical Climate Variability and Long-term Trend Influences on U.S. Temperature and Precipitation Forecasts for Weeks 3 and 4

Daniel S. Harnos¹, Nathaniel C. Johnson^{2,3}, Stephen R. Baxter¹,
Michelle L. L'Heureux¹, and Adam D. Allgood¹

¹*Climate Prediction Center, NOAA/NWS/NCEP, College Park, Maryland*

²*Geophysical Fluid Dynamics Laboratory, NOAA, Princeton, NJ*

³*Department of Atmospheric and Oceanic Sciences, Princeton University, Princeton, NJ*

1. Introduction

The Climate Prediction Center (CPC) began issuing probabilistic, two-class forecasts of 2-meter temperature (T_{2m}) and precipitation (P) for the combined weeks 3-4 period (days 15-28) in September 2015. This product serves to bridge the gap between traditional extended range forecasts (days 8-14) and monthly forecasts. The week 3-4 period has been typically thought to be one of low forecast skill, due to insufficient time for boundary conditions to take hold on a forecast, while dynamical guidance suffers from substantial growth of initialization errors.

While dynamical model guidance will always play a substantial role in forecasting, statistical methods can potentially exploit signals from the initial climatic state that can uniquely inform subseasonal forecasters. For example, Riddle *et al.* (2013) and Baxter *et al.* (2014) revealed impacts of the Madden-Julian Oscillation (MJO) through subseasonal timescales on the circulation and T_{2m} of North America. Johnson *et al.* (2014) used a compositing method (detailed in next section) to support that non-linear combined influences of MJO, long-term trend, and the El Niño-Southern Oscillation (ENSO) could often produce skillful week 3-4 wintertime U.S. T_{2m} forecasts. This work seeks to extend Johnson *et al.* (2014) to all seasons while incorporating P forecasts, and also to explore the impacts of ENSO/MJO linearity/non-linearity on week 3-4 forecasts.

2. Data and methodology

Training and cross-validation data for T_{2m} (Janowiak *et al.* 1999) and P (Xie *et al.* 2010) are taken over running 3-month periods between 1982-2013 to evaluate days 15-28, with these same datasets utilized for verification purposes. ENSO information is utilized in the form of the Oceanic Niño Index (3-month running mean Niño 3.4 region SST anomaly) and the daily Real-time Multivariate MJO (RMM; Wheeler and Hendon 2004) index to characterize the MJO.

The first methodology to investigate Week 3-4 predictability of T_{2m} and P is the so-called “phase model” (PM) of Johnson *et al.* (2014), which closely follows traditional compositing methods. In short, mean and variance shifts are quantified based upon the historical 15-28 day distributions of T_{2m} and P for subsets of ENSO (three states - El Niño, Neutral, or La Niña following typical conventions), and the MJO (nine states – one for each conventional phase and another when the amplitude is < 1), with an additional mean shift associated with linear long-term trend. A Gaussian probability density function (PDF) is assumed for the forecast distribution, with a fourth root transform utilized to increase normality for P , where the summed means (ENSO, MJO, and trend) and variances (ENSO and MJO) build the forecast PDF. This PDF can then be compared to the climatological median values, to evaluate what proportion of the forecast distribution are above- and below-normal.

While the former method yields differences in the forecast state based on ENSO, MJO, and trend it can often have abrupt forecast discontinuities when transitioning between climatic states (*e.g.* MJO phases 4, 5, or a weak MJO) while the solutions also fail to scale for potential impacts sourced from the amplitude of the

background climate state. These shortcomings can be addressed through a multiple linear regression (MLR) framework, with predictands of T_{2m} and P and standardized predictors of: RMM1 and RMM2 for MJO, the 2-week mean Nino 3.4 anomaly from OISSTv2 (Reynolds et al. 2007) for ENSO, and a daily index for linear long-term trend. The regression relationship is used to determine the mean shifts in the day 15-28 T_{2m} and P distributions based on the initial climatic state, while the climatological variance is used in conjunction with a skill correction then used to build a Gaussian forecast PDF. This PDF is then evaluated with respect to climatological values, as with the PM.

All skill evaluations utilize the Heidke Skill Score (HSS), which is the difference of the number of correct forecasts and number of forecasts to be expected to be randomly correct (50% in a two-class forecast), divided by the difference of the total number of forecasts and number of forecasts expected to be randomly correct. The HSS can range over ± 100 , with a score of 0 indicating no improvement relative to random chance while positive values indicate added value. Cross-validation is performed using a leave-one-year out methodology.

3. Cross-validation performance

Cross-validation reveals both the PM and MLR on average across the U.S. are largely, and often significantly, skillful across a breadth of many initial ENSO and MJO states in multiple seasons for both T_{2m} (Fig. 1) and P (Fig. 2). For each predictand, embedded periods of enhanced predictability, evidenced by marked increases in HSS, or “forecasts of opportunity” exist (e.g. MJO phases 2-5 with a background La Niña during FMA). Also notable is that skill

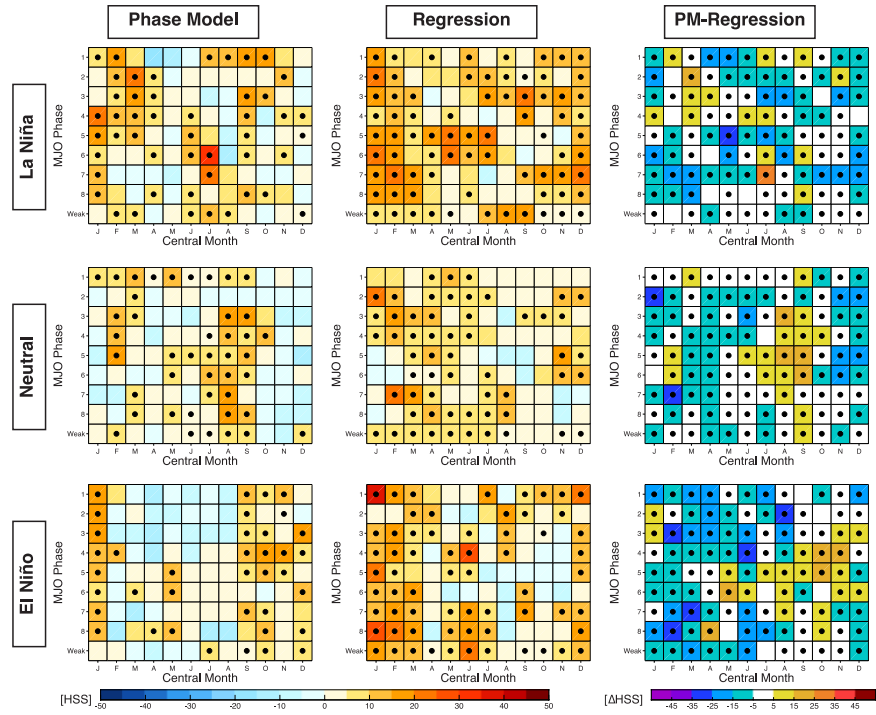


Fig. 1 Hindcast T_{2m} HSS spatially averaged for all U.S. grid cells via the PM (left column), MLR (center column) and difference between the two (right column) across MJO/ENSO base states and running 3-month period. Dots indicate statistical significance $\geq 95\%$ via Monte Carlo Simulation.

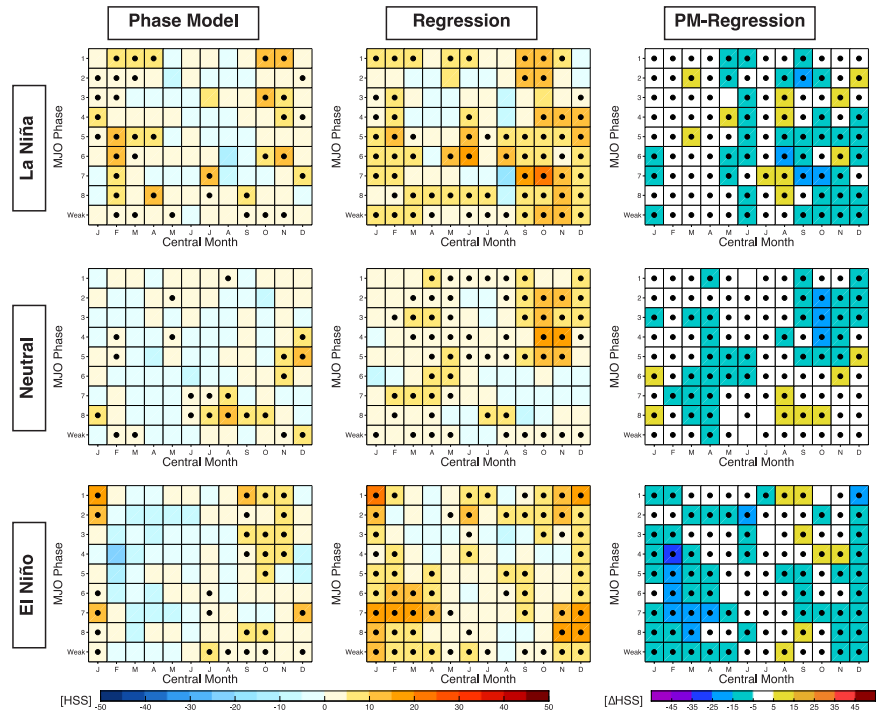


Fig. 2 As in Figure 1, but for P .

exists across a wide range of ENSO and MJO states, and is often significantly higher than the skill of the PM and MLR models.

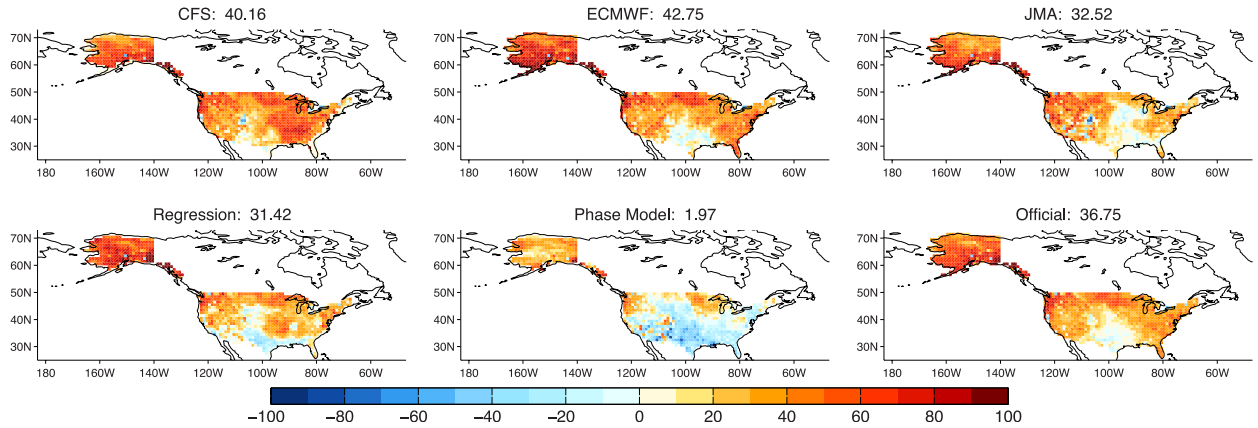


Fig. 3 T_{2m} HSS values for the listed dynamical and statistical guidance and official CPC outlooks. U.S. average values shown in panel titles.

often exists in the absence of an active MJO and non-neutral ENSO state, including for P , where trends are assumed to hold a lesser impact.

Comparisons can also be made between the relative performance of the PM and MLR, relating to the underlying assumptions used in building each statistical model (rightmost column of Figs. 1 and 2). In general, the MLR (cooler colors) outperforms the PM (warmer colors) with the exception of late (early) boreal summer (autumn). These differences between the two methodologies are generally statistically significant in both T_{2m} and P . This implies that the magnitude of large-scale teleconnections generally holds importance, and the linear assumption is reasonably well founded as utilized in the regression forecast. This also suggests that the importance of predictand mean shifts in the forecast PDFs dwarfs that of variance shifts within MJO and ENSO states, as there is no variance adjustment relative to climatology in the MLR, whereas the PM does account for variance differentiation dependent upon the initial state. Given the typically superior performance of the MLR relative to the PM and the similar drivers of each statistical method, it is reasonable to question about the necessity of the PM. While rooted in similar information, the differing methodologies of the MLR and PM can often yield differing probabilistic forecasts for geographic regions, while one method is skillful and the other lacks skill (not shown) where the tool with greater HSS can be emphasized.

4. Real-time performance

Results are presented here for the statistical guidance along with bias-corrected dynamical model ensemble guidance from several sources (CFSv2, ECMWF, and JMA) and official CPC outlooks for the “real-time” period since CPC began issuing Week 3-4 outlooks (18 September, 2015 - 8 July, 2016). HSS values are reported for all grid points (*i.e.* equal chances in the official CPC outlooks have 50% taken as hits and misses to create a consistent point of comparison with guidance products the encompass all points).

Figures 3 and 4 show the HSS values at the grid point level for T_{2m} and P respectively over the real-time period for the five guidance sources and official CPC outlooks. For T_{2m} , HSS values are shown to be largely skillful, with domain average values typically in the 30-40 range, indicative of 65-70% of forecasts being in the correct category relative to normal. For P , HSS values are lower with domain averages typically in the ± 5 range, values that are likely not robust given limited sample for the real-time period. The worst performing forecast over the real-time period in both T_{2m} and P comes from the PM, likely due to the lack of canonical El Niño impacts observed during 2015-2016. Interestingly, the MLR seems to not suffer from the lack of typically observed ENSO impacts and performs closely to, or sometimes better than, dynamical model guidance and the official CPC outlooks.

In evaluating Figures 3 and 4 one notes the consistent regions of high HSS (for T_{2m} it is widespread outside the Southern Plains, for P it is focused in Alaska and the Northern/Central Plains) and low HSS (for T_{2m} the Southern Plains, for P the Southwest) for all forecasts with the exception of the PM. It is worth exploring whether there are possible co-dependent relationships between the dynamical and statistical

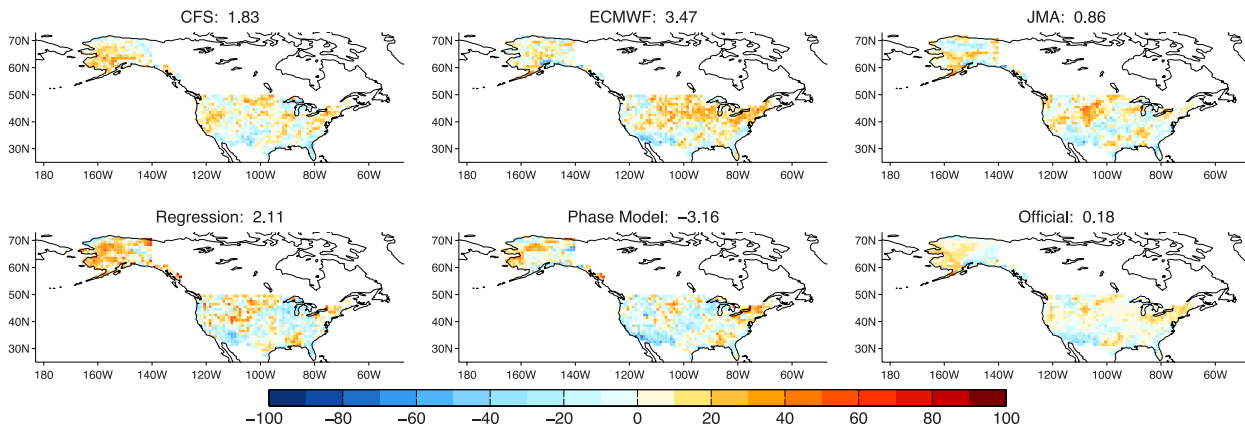


Fig. 4 As in Figure 3 but for P .

guidance, with the official outlooks having a clear dependency given that they are based on the aforementioned guidance. Figure 5 shows the time series of HSS spatially averaged across the U.S. for each of the forecast products over the real-time period. With the exception of the PM for T_{2m} it is apparent that dynamical and statistical guidance tends to cluster closely together on a weekly basis. Combined with Figures 3 and 4, these analyses suggest limited novel information between the dynamical models and ENSO/MJO/trend-based statistical guidance for the Week 3-4 timeframe. An analysis of the correlation coefficient at the grid-scale level of the forecast probabilities for T_{2m} and P of the weekly dynamical model forecasts with the MLR for the real-time period reveals several broad regions with values ≥ 0.6 (not shown). For T_{2m} these regions vary, and appear closely tied to dynamical model representation of long-term trend, while for P the highly correlated regions are focused in the west and south, regions where ENSO has a substantial footprint. Altogether, such analyses suggest limited novel information being provided from dynamical model guidance relative to the ability of the ENSO/MJO/trend baseline to characterize variance, and instead the model forecasts appear to be largely derived upon the model's representation of impacts from the latter modes of variability. Future work should seek to explore the utility of dynamical model guidance across climate timescales relative to background climate states, such as the three modes explored here at subseasonal periods, or ENSO and trend for the seasonal timeframe.

Acknowledgements. This project was funded by the NOAA/CPO MAPP program. We appreciate the respective forecast centers for supplying their dynamical model ensemble guidance. Augustin Vintzileos and Dan Collins respectively post-processed the CFS and JMA.

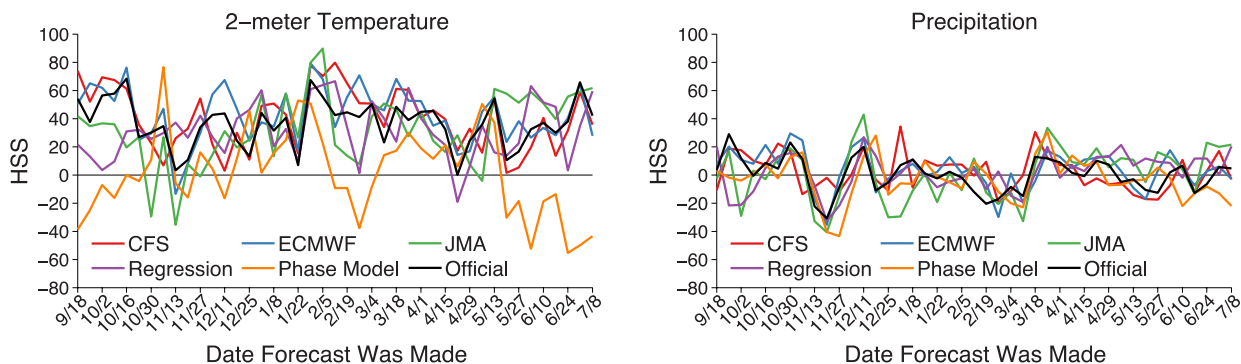


Fig. 5 Time series of U.S. averaged HSS for T_{2m} (left) and P (right).

References

Baxter, S., S. Weaver, J. Gottschalck, and Y. Xue, 2014: Pentad evolution of wintertime impacts of the Madden-Julian Oscillation over the Contiguous United States. *J. Climate*, **27**, 7356-7367.

-
- Janowiak, J., G. Bell, and M. Chelliah, 1999: A gridded database of daily temperature maxima and minima for the conterminous US: 1948-1993. *NCEP/CPC Atlas 6*, Natl. Cent. For Environ. Predict., Camp Springs, MD.
- Johnson, N. C., D. C. Collins, S. B. Feldstein, M. L. L'Heureux, and E. E. Riddle, 2014: Skillful wintertime North American temperature forecasts out to 4 weeks based on the state of ENSO and the MJO. *Wea. Forecasting*, **29**, 23-38.
- Reynolds, R. W., T. M. Smith, C. Liu, D. B. Chelton, K. S. Casey, and M. G. Schlax, 2007: Daily high-resolution-blended analyses for sea surface temperature. *J. Climate*, **20**, 5473-5496.
- Riddle, E. E., M. B. Stoner, N. C. Johnson, M. L. L'Heureux, D. C. Collins, and S. B. Feldstein, 2013: The impact of the MJO on clusters of wintertime circulation anomalies over the North American region. *Clim. Dyn.*, **40**, 1749-1766.
- Wheeler, M. C. and H. H. Hendon, 2004: An all-season real-time multivariate MJO index: Development of an index for monitoring and prediction. *Mon. Wea. Rev.*, **132**, 1917-1932.
- Xie, P., M. Chen, and W. Shi, 2010: CPC unified gauge-based analysis of global daily precipitation. Preprints, *24th Conf. on Hydrology*, Atlanta, GA, Amer. Meteor. Soc., 2.3A. (Available online at http://ams.confex.com/ams/90annual/techprogram/paper_163676.htm.)